ELSEVIER

Thermochimica Acta 265 (1995) 15–23

thermochimica acta

Calorimetric investigation on the formation of gold nanoparticles in water/AOT/*n*-heptane microemulsions

F. Aliotta [a], V. Arcoleo [b], S. Buccoleri [c], G. La Manna [c], V. Turco Liveri [b,*]

[a] *Istituto Tecniche Spettroscopiche, CNR, Messina, Italy*
[b] *Dipartimento di Chimica Fisica, Palermo, Italy*
[c] *Dipartimento di Biologia Cellulare e dello Sviluppo, Palermo, Italy*

Received 31 October 1994; accepted 20 March 1995

Abstract

The formation enthalpy of gold nanoparticles in water/sodium bis(2-ethylhexyl) sulfosuccinate (AOT)/*n*-heptane microemulsions as a function of the water/AOT molar ratio $R(R = [\text{water}]/[\text{AOT}])$ was measured by a calorimetric technique at various AOT concentrations. The size of Au nanoparticles was determined by transmission electron microscopy. The results indicate that both the energetic state and the dimensions of the gold nanoparticles are influenced by the radius and the concentration of the reversed AOT micelles. Analysis of the decay of the calorimetric signal provides evidence of some interesting features of the growing process of the Au nanoparticles in water/AOT/*n*-heptane microemulsions.

Keywords: Calorimetry; Formation enthalpy; Gold nanoparticles; Micelles; Microemulsions

1. Introduction

Nowadays, the production and the characterization of nanoparticles is a very active field of investigations [1, 2] mainly because materials with new and interesting properties can be realized by simply reducing their size to the nanometer scale.

Among the various methods used to obtain nanoparticles, a promising one is based on the use of water-in-oil microemulsions as suitable solvent and reaction media [3, 4]. These systems have, in fact, ideal structural and dynamic properties: they are made up of surfactant-stabilized water nanodroplets (radius 0–200 Å) dispersed in an organic

* Corresponding author.

0040-6031/95/$09.50 © 1995 – Elsevier Science B.V. All rights reserved
SSDI 0040-6031(95)02411-5

solvent of low polarity which continuously exchange material with each other [5–7]. This exchange process [8] enables hydrophilic reactants solubilized in different water nanodroplets to come in contact and react wheras their closed structure and dispersion in the system represents an obstacle for unconditional particle growth.

Among the various techniques (small angle X-ray scattering, UV–Vis spectrophotometry, transmission electron microscopy and light scattering) [9] employed to investigate effectively the formation of metal colloids in microemulsions it has been shown that microcalorimetry is a sensitive technique particularly useful for providing evidence of the energetic state and growing process of nanoparticles [4,10]. In particular, a previous investigation on the formation of palladium nanoparticles in water/AOT/*n*-heptane microemulsions allowed us to show that the enthalpy of formation of Pd in microemulsions is significantly different from that in water, and that the dimensions of the Pd nanoparticles are not regulated by the water nanodroplet radius r_w ($r_w = 1.8R$; R = [water]/[AOT]) [5] but result from a delicate equilibrium between the spontaneous tendency of the nanoparticles to grow and the energetically unfavorable blowing up of the reversed micelles [11].

Given the importance of finely subdivided metallic particles, we decided to extend our investigations to the formation of Au nanoparticles in water/AOT/*n*-heptane

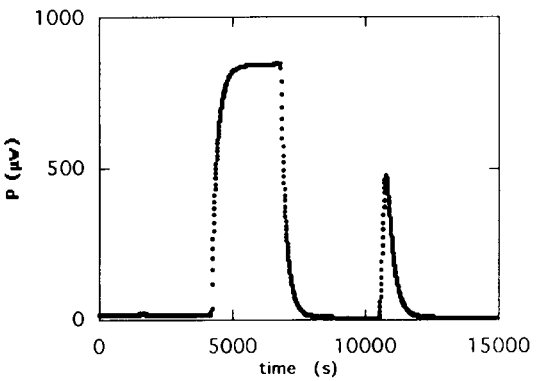

Fig. 1. Typical calorimetric signal vs time curve. (The first signal is the calibration curve, the second refers to the system at $R = 15$ and [AOT] = 0.15).

Table 1
Molar enthalpies (ΔH_{exp}/kJ mol^{-1}) of Au formation as a function of R at various AOT concentrations

[AOT] = 0.15		[AOT] = 0.32		[AOT] = 0.40		[AOT] = 1.0	
R	ΔH_{exp}	R	ΔH_{exp}	R	ΔH_{exp}	R	ΔH_{exp}
3	−246	3	−260	3	−280	5	−375
8	−300	5.2	−305	5	−320	8	−460
15	−360	10	−371	10	−401	10	−480
		15	−420	15	−506		

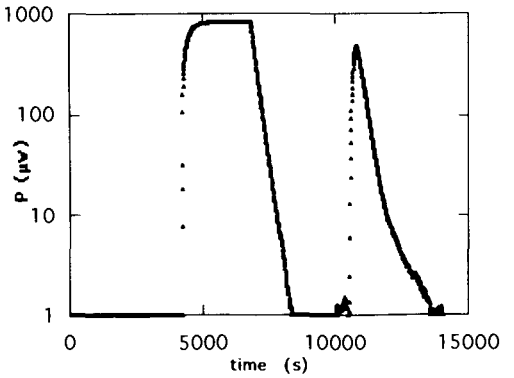

Fig. 2. Semilogarithmic plot of the calorimetric signal vs time curve. (The first signal is the calibration curve, the second refers to the system at $R = 15$ and [AOT] = 0.15).

microemulsions. Gold nanoparticles were obtained in situ reduction of tetra-chloroauric(III) acid by hydrazine sulfate. Since both reagents are hydrophilic, it must be expected that they are located in the aqueous core of the AOT reversed micelles.

2. Experimental

2.1. Materials

Sodium bis(2-ethylhexyl) sulfosuccinate (AOT; Sigma, 99%), tetrachloroauric(III) acid ($HAuCl_4$, Sigma, 49% Au), hydrazine sulfate ($N_2H_4 \cdot H_2SO_4$, Fluka, > 99%) and

Table 2
Time constants (τ_1. τ_2) for the formation of Au nanoparticles in water/AOT/*n*-heptane microemulsions as a function of R at various AOT concentrations

R	[AOT]	τ_1/s	τ_2/s
3	0.15	220	435
8	0.15	290	510
15	0.15	241	621
3	0.32	255	395
5	0.32	262	610
10	0.32	240	595
15	0.32	245	706
3	0.40	285	450
5	0.40	290	480
10	0.40	300	590
15	0.40	310	600
5	1.0	435	869
8	1.0	410	920
10	1.0	430	1050

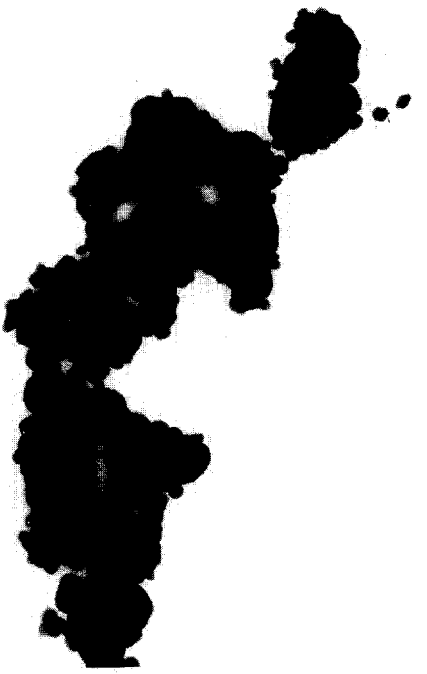

Fig. 3. Electron micrograph of Au nanoparticles from precipitate of microemulsion at $R = 5$ and [AOT] = 0.32 (dimension of nanoparticles about 200 Å).

n-heptane (Merck, > 99%) were used as received. All the solutions were prepared by weight by dissolving appropriate amounts of a 0.023 M aqueous solution of $HAuCl_4$ or a 0.13 M aqueous solution of $N_2H_4 \cdot H_2SO_4$ in AOT/*n*-heptane solution at various AOT molar concentrations ([AOT] = 0.15; 0.32; 0.40; 1.0).

2.2. Methods

Calorimetric measurements were performed at 25°C using a "Thermal Activity Monitor" (TAM) produced by LKB (LKB 2277) equipped with a mix-flow cylinder (LKB 2277-204) and a perfusion cell (LKB 2277-402). A typical run was carried out as follows. A known amount (about 1.5 g) of microemulsion containing $HAuCl_4$ was placed in the perfusion cell. This cell was inserted into the calorimeter and, after thermal equilibration, an amount (150–200 μl) of a microemulsion containing $N_2H_4 \cdot H_2SO_4$ was added by an injection cannula connected to a Hamilton syringe. In order to avoid heat effects due to variation of the molar ratio R (R = [water]/[AOT]) and/or of the

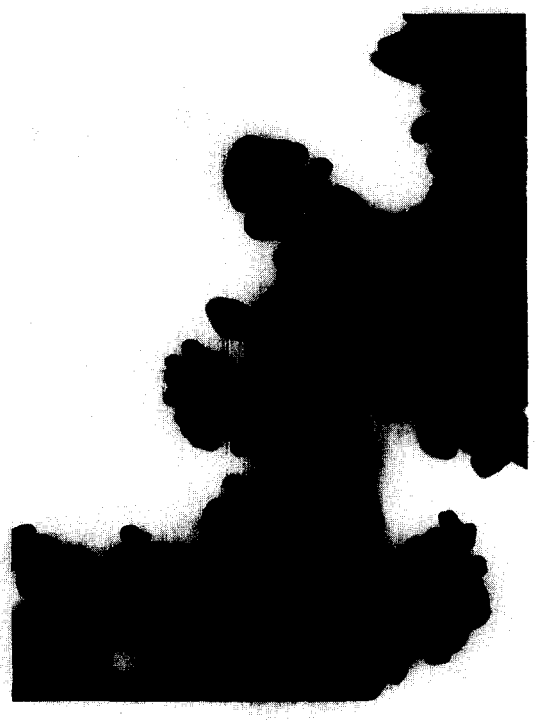

Fig. 4. Electron micrograph of Au nanoparticles from supernatant of microemulsion at $R = 15$ and [AOT] = 0.15 (dimension of nanoparticles about 320 Å).

AOT concentration, each experiment was carried out by mixing microemulsions having the same values of these parameters [12].

Fig. 1 shows a typical calorimetric signal vs time plot together with the calibration signal. The experimental enthalpies (estimated uncertainty $\pm 0.5\%$) were obtained through the integrated area under these curves. The molar enthalpies (ΔH_{exp}) of Au formation in the investigated samples are reported in Table 1.

Another feature of the calorimetric signal (P) vs time plots can be appreciated if one reports the logarithm of P vs time (see Fig. 2). As can be seen, after an initial quite instantaneous increase, this quantity shows a decay characterized by two linear trends. This means that each trend can be fitted by a first order rate process equation [13, 14]

$$P \propto e^{-t/\tau} \tag{1}$$

where t is the time and τ is a time constant simply related to the rate constant (k) of the process ($\tau = 1/k$). Thus, by analyzing the decay curve, it is possible to obtain two time constants (τ_1, τ_2) which can be used to provide kinetic information if the processes have a time constant (τ) greater than that (τ_S) of the microcalorimeter [11]. τ_S, obtained by

Fig. 5. Electron micrograph of Au nanoparticles from supernatant of microemulsion at $R = 15$ and [AOT] = 0.32 (dimension of nanoparticles about 450 Å).

analyzing the decay of the calibration signal, was 200 s (a value of 140–330 s is reported in the LKB application notes). The values of τ_1 and τ_2 obtained by fitting the decay curves through Eq. (1) are reported in Table 2.

At the end of each experiment, the samples were visually inspected. For all the samples, a thin gold precipitate was observed at the bottom of the calorimetric cell. Observation of this precipitate with a transmission electronic microscope (Philips, EM420) surprisingly showed that it comprised gold nanoparticles (see Fig. 3). This finding indicates that Au nanoparticles, most probably stabilized by a layer of surfactant molecules, can cluster together forming very big aggregates which, above a threshold dimension, precipitate. Nanoparticles were also found in the supernatant. They were observed by transmission electron microscopy after gentle evaporation of the solvent (see Figs. 4 and 5).

3. Results and discussion

Fig. 6 shows the trends of the molar enthalpies (ΔH_{exp}) of Au formation as a function of R. These trends, similar to that previously observed for the formation of palladium

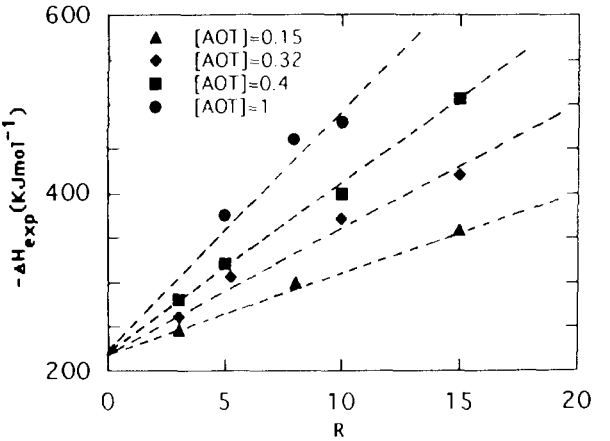

Fig. 6. Experimental molar enthalpies of formation of Au nanoparticles as a function of the ratio R at various AOT concentrations. (Lines are only a guide for the eye.)

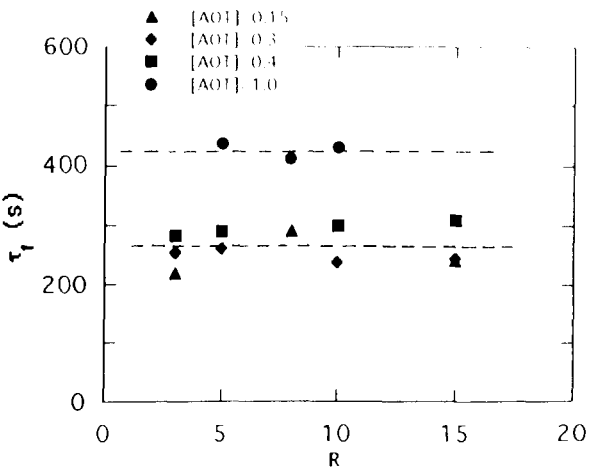

Fig. 7a. Time constant of the first process as a function of R at various AOT concentrations. (Lines are only a guide for the eye.)

nanoparticles in the same system [11], can be consistently explained in terms of formation of nanoparticles. In a nanoparticle, in fact, the fraction of surfacial atoms is significant and their energetic state higher than that in the core. It follows that, by decreasing the nanoparticle size, the enthalpy of formation of nanoparticles is expected to become progressively less negative (i.e., a less exothermic process). On the other hand, it can be reasonably expected that by decreasing R (i.e., at lower micellar radius) smaller nanoparticles are formed. In accordance with this interpretation, the observed dependence of ΔH_{exp} upon [AOT] indicates that smaller nanoparticles are formed at

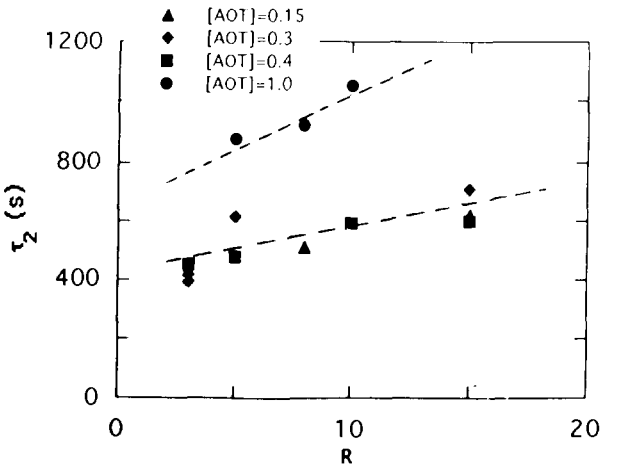

Fig. 7b. Time constant of the second process as a function of R at various AOT concentrations. (Lines are only a guide for the eye.)

lower AOT concentrations. This was directly confirmed by electron microscopy. In fact, nanoparticles with a mean radius of 200 Å were obtained in microemulsions at $R = 5$ and [AOT] = 0.32, whereas at $R = 15$ the mean radius was 320 Å at [AOT] = 0.15 and 450 Å at [AOT] = 0.32. It must be pointed out that nanoparticles of the same dimensions were found in samples obtained from the sediment or from the supernatant of the same microemulsion. Moreover, it must be noted that the radius of the nanoparticles is significantly greater than the micellar radius (r_w) ($r_w = 9$ Å at $R = 5$, $r_w = 27$ Å at $R = 15$). This finding, similar to that previously observed for the formation of Pd nanoparticles [11], can be rationalized in terms of a competition between two opposite tendencies (the spontaneous tendency of nanoparticles to grow, and the spontaneous tendency of reversed micelles to maintain their radius). The adsorption of the surfactant at the surface of the nanoparticles could have a role on the stabilization mechanism of nanoparticles [15] and could also contribute to their enthalpy of formation. Since our calorimetric and microscopic results indicate that by increasing [AOT] (i.e., the concentration of the AOT reversed micelles) the nanoparticle dimensions increase, it can be argued that the collisional frequency among reversed micelles play a significant role in the nanoparticle formation process.

In Fig. 7 the time constants (τ_1, τ_2) are shown as a function of R. As can be seen, for both parameters, only at [AOT] = 1 did we observe values which differ from those observed at lower AOT concentrations. Moreover, by increasing R, a slight increase of τ_2 and nearly constant τ_1 are observed. Even if it is reasonable to attribute the time constants to two consecutive processes involving Au nanoparticles, the small set of data and the complexity of the phenomena connected with the nanoparticle formation suggest caution. However, as a working hypothesis, we could propose that the first process is the formation of Au nuclei within the AOT reversed micelles and the second is a slower process consisting in the formation of aggregates of surfactant-stabilized Au nanoparticles.

Acknowledgement

This work has been supported by the Italian Council Researches (CNR) and by MURST.

References

[1] G. Schmid, Chem. Rev., 92 (1992) 1709.
[2] C. Petit, P. Lixon and M.P. Pileni, J. Phys. Chem., 94 (1990) 1598.
[3] J.H. Fendler, Chem. Rev., 87 (1987) 877.
[4] A. D'Aprano, F. Pinio and V. Turco Liveri, J. Solution Chem., 20 (1991) 301.
[5] J. Eastoe, G. Fragneto, B.H. Robinson, T.F. Towey, R.K. Heenen and F.J. Leng, J. Chem. Soc. Faraday Trans. 1, 88 (1992) 461.
[6] P.D.I. Fletcher and B.H. Robinson, Ber. Bunsenges Phys. Chem., 85 (1981) 863.
[7] G. D'Arrigo, A. Paparelli, A. D'Aprano, I.D. Donato, M. Goffredi and V. Turco Liveri, J. Phys. Chem., 93 (1989) 8367.
[8] P.D.I. Fletcher, A.M. Howe and B.H. Robinson, J. Chem. Soc. Faraday Trans. 1, 83 (1987) 985.
[9] M.A. Lopez-Quintela and J. Rivas, J. Colloid Interface Sci., 158 (1993) 446.
[10] V. Arcoleo, M. Goffredi and V. Turco Liveri, Thermochim. Acta, 233 (1994) 187.
[11] V. Arcoleo, G. Cavallaro, G. La Manna and V. Turco Liveri, Thermochim. Acta, 254 (1995) 111.
[12] A. D'Aprano, A. Lizzio and V. Turco Liveri, J. Phys. Chem., 91 (1987) 4749.
[13] A. Buzzell and J.M. Sturtevant, J. Am. Chem. Soc., 73 (1951) 2454.
[14] C.H. Lueck, L.F. Beste and H.K. Hall, J. Am. Chem. Soc., 67 (1963) 972.
[15] M. Boutonnet, J. Kizling, P. Stenius and G. Maire, Colloids Surfaces, 5 (1982) 209.